Structure, Vol. 12, 1067–1077, June, 2004, ©2004 Elsevier Ltd. All rights reserved. DOI 10.1016/j.str.2004.02.040

The Structure of MSK1 Reveals a Novel Autoinhibitory Conformation for a Dual Kinase Protein

Kathrine J. Smith,[1,*] Paul S. Carter,[1] Angela Bridges,[1] Pete Horrocks,[1] Ceri Lewis,[1] Gary Pettman,[1] Andrew Clarke,[3] Murray Brown,[3] Jane Hughes,[2] Marc Wilkinson,[2] Benjamin Bax,[1] and Alastair Reith[3]

[1]Discovery Research
[2]Neurology Centre of Excellence in Drug Discovery
GlaxoSmithKline
Third Ave
Harlow, Essex, CM19 5AW
United Kingdom
[3]Discovery Research
GlaxoSmithKline
Gunnels Wood Road
Stevenage, Hertfordshire, SG1 2NY
United Kingdom

Summary

Mitogen and stress-activated kinase-1 (MSK1) is a serine/threonine protein kinase that is activated by either p38 or p42ERK MAPKs in response to stress or mitogenic extracellular stimuli. MSK1 belongs to a family of protein kinases that contain two distinct kinase domains in one polypeptide chain. We report the 1.8 Å crystal structure of the N-terminal kinase domain of MSK1. The crystal structure reveals a unique inactive conformation with the ATP binding site blocked by the nucleotide binding loop. This inactive conformation is stabilized by the formation of a new three-stranded β sheet on the N lobe of the kinase domain. The three β strands come from residues at the N terminus of the kinase domain, what would be the αB helix in the active conformation, and the activation loop. The new three-stranded β sheet occupies a position equivalent to the N terminus of the αC helix in active protein kinases.

Introduction

Mitogen and stress activated kinase 1 (MSK1) is a serine/threonine kinase that is activated in response to both growth factor and cellular stress stimuli (Deak et al., 1998; Pierrat et al., 1998; New et al., 1999; Markou and Lazou, 2002). MSK1 belongs to a family of protein kinases that contain two protein kinase domains in one polypeptide chain (Figure 1A). Other kinases that belong to this family of dual kinase proteins include the MAPKAP-K1/p90R^{RSK} family of proteins and MSK2 (Deak et al., 1998). Of these proteins, MSK2 is a closely related homolog of MSK1 with overall sequence identity of approximately 75%. Aside from MSK2, MSK1 is most closely related to the relatively well-characterized protein MAPKAP-K1/RSK2 (43% sequence identity). Both MSK1 and MAPKAP-K1 act downstream of the MAPK level of kinases. Unlike MAPKAP-K1, which is responsive only to ERK, MSK1 has been shown to be a cellular substrate of both the ERK and p38 MAP kinase pathways (Deak et al., 1998; Pierrat et al., 1998; New et al., 1999) and so likely serves to integrate signals transduced from distinct extracellular stimuli. As such, we would expect MSK1 to be subject to regulation of activity by a variety of mechanisms, including conformational state. In contrast to MAPKAP-K1, which is found in both the cytoplasm and the nucleus, MSK1 has been reported to exist exclusively in the nucleus (Zhao et al., 1995; Chen et al., 1992; Deak et al., 1998). Consistent with its nuclear location, MSK1 has been shown to phosphorylate a range of substrates including the transcription factor CREB in response to stress stimuli (Deak et al., 1998; Arthur and Cohen, 2000; Wiggen et al., 2002) and has been implicated in CREB-mediated transcriptional regulation of IL-1β and COX-2. MSK1 has also been reported to phosphorylate and activate the transcription factor NFκb (Vermeulen et al., 2003) and regulate the activity of ER81 and MUC5AC (Janknecht, 2003; Song et al., 2003). In addition to transcription factors, MSK1 has also been reported to phosphorylate the nucleosomal proteins histone H3 and HMG-14 (Thompson et al., 1999; Zhong et al., 2003).

In the dual domain protein kinase MAPKAP-K1, the N-terminal kinase has been shown to phosphorylate exogenous substrates, while the C-terminal kinase and the linker region act to regulate activity of the N-terminal kinase (Bjorbaek et al., 1995; Dalby et al., 1998; Vik and Ryder, 1997). Interestingly, MAPKAP-K1 is activated by autophosphorylation as well as phosphorylation from upstream kinases. It has been shown that MAPKAP-K1 is activated by phosphorylation of four key residues, Ser222, Ser364, Ser381, and Thr574 (Dalby et al., 1998) (Figure 1A shows the equivalent residues in MSK1). Ser222 and Thr574 are located on the activation loops of the N- and C-terminal kinase domains respectively, while Ser364 and Ser381 are located in the linker region, joining the two kinase domains. Ser381 is located in a hydrophobic motif conserved among a large number of the AGC family of kinases (Pearson et al., 1995; Frodin et al., 2002). ERK has been shown to activate the C-terminal kinase of MAPKAP-K1 by phosphorylation of Thr571 and Ser364 (Fisher and Blenis, 1996; Dalby et al., 1998). The activated C-terminal kinase then phosphorylates Ser381 in the linker region (Vik and Ryder, 1997). This serves as a docking site for PDK1, which then fully activates MAPKAP-K1 by phosphorylation of Ser222 in the N-terminal kinase domain (Jensen et al., 1999; Richards et al., 1999; Williams et al., 2000; Frodin et al., 2000). MSK1 is believed to be activated in a similar way to MAPKAP-K1 (Figure 1A). The four key phosphorylation sites are conserved between the two proteins, and MSK1 residue Ser376 is located in a conserved hydrophobic motif in the linker region (Deak et al., 1998; Frodin et al., 2000, 2002). In contrast to MAPKAP-K1,

*Correspondence: kathrine_j_smith@gsk.com

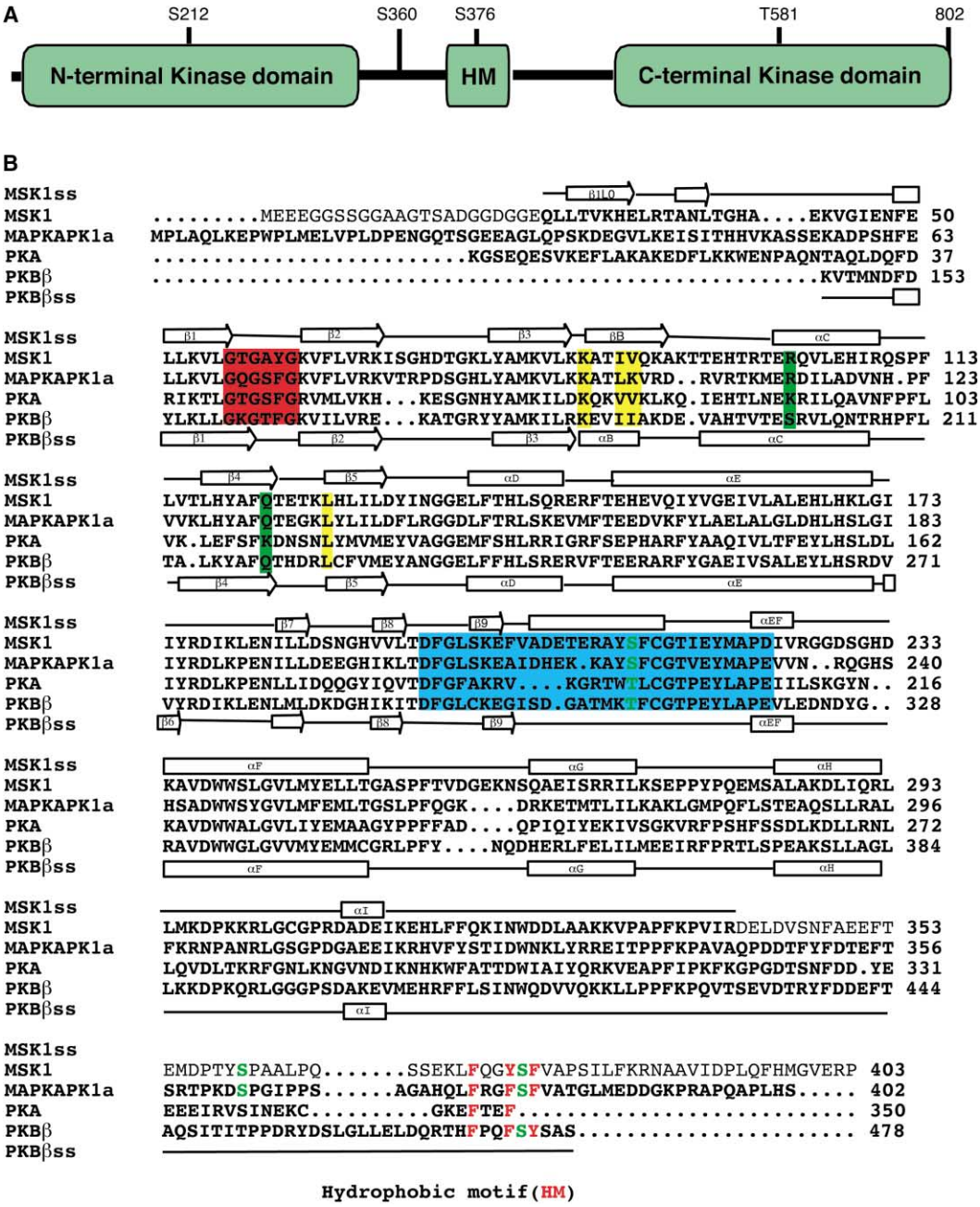

Figure 1. Schematic Picture of Full-Length MSK1 and Sequence Alignment of the N-terminal Domain

(A) is a schematic diagram of full-length MSK1, showing the four putative phosphorylation sites (S212, S360, S376, and T581), the linker region between the two kinase domains and the hydrophobic motif (HM).

(B) is a sequence alignment of MSK1 N-terminal domain and linker region (residues 1–403), with MAPKAP-K1a, PKA, and PKBβ. On the MSK1 sequence the residues observed in the crystal structure are shown in bold. The secondary structure (ss) of MSK1 and PKBβ are shown above and below the alignment. The nucleotide binding loop of the three proteins is highlighted in red and the activation loop is highlighted in blue. Residues highlighted in yellow are residues conserved in the hydrophobic binding groove; residues highlighted in green are conserved residues in the phosphoserine/threonine docking site. The phosphorylation sites S212, S260, and S376 are shown in green font. The hydrophobic motif (HM) is also shown on the alignment.

Note: MSK1 is also known as Ribosomal protein S6 kinase α5, RPS6KA5.

which is phosphorylated by PDK1, MSK1 is believed to autophosphorylate Ser212, in the activation loop of the N-terminal kinase (Williams et al., 2000). Phosphorylation of residues in the activation loop is a common mechanism for activating protein kinases (Johnson et al., 1996).

The N-terminal kinase domains of MSK1, MSK2, and MAPKAP-K1 are members of the structurally related AGC

family of protein kinases which include p70 ribosomal S6 kinase (S6K), serum and glucocorticoid-induced kinase (SGK), protein kinase A (PKA), and protein kinase B (PKB) (Figure 1B). Crystal structures of active-like conformations of four AGC family kinases (Knighton et al., 1991; Biondi et al., 2002; Yang et al., 2002b, Lodowski et al., 2003) all have an αB helix in the N-terminal lobe of the kinase that helps to form part of a functionally important hydrophobic groove (this structural feature seems to be specific to AGC family kinases). The hydrophobic groove serves as a binding site for a hydrophobic motif (F-x-x-F-[S/T]-Y) (Pearson et al., 1995). Phosphorylation of the serine or threonine residue in the hydrophobic motif has been shown to be important for either intramolecular or intermolecular regulation of the activity of many AGC family kinases. Recent crystal structures of active and inactive forms of PKB have revealed how phosphorylation of Ser474 in the C-terminal hydrophobic motif is responsible for a disorder to order transition in the αB and αC helices (which form two sides of the "hydrophobic groove") and the intramolecular activation of this protein kinase (Yang et al., 2002a, 2002b; Huang et al., 2003). In contrast, the phosphorylated hydrophobic motif has been shown to act as a docking site for PDK1 in PDK1 target kinases, for example MAPKAP-K1/RSK2 (Frodin et al., 2000), PRK2, PKCζ (Balendran et al., 2000), and SGK1 (Biondi et al., 2000), thus serving as a mechanism of intermolecular activation. Recent mutational and modeling studies carried out with a number of AGC family kinases, including MSK1, have demonstrated the importance of the hydrophobic pocket and phosphoserine/threonine binding site in mediating activation via hydrophobic motif phosphorylation (Frodin et al., 2002).

This paper describes the crystal structure of the N-terminal kinase domain of MSK1. The structure reveals a novel autoinhibitory conformation where the hydrophobic pocket is disrupted by a unique β sheet structure. The β sheet is composed of residues from the protein N terminus, what would be the αB helix in an active kinase, and the β9 strand from the activation segment. Sequence analysis and comparison with the conformation of an active kinase suggests that activation of MSK1 requires significant structural rearrangement of the N-terminal domain and formation of the hydrophobic binding pocket/phosphoserine/threonine binding site. We propose that (similar to active PKB) the active form of MSK1 assumes a conformation in which the phosphorylated hydrophobic motif, in the linker region between the two kinase domains, binds in the hydrophobic binding pocket/phosphoserine/threonine binding site on the N-terminal domain.

Results

Activity Analysis and Structure Determination

The N-terminal kinase domain of MSK1 (1-350, S212D) was expressed and purified using a Baculovirus expression system (Figure 2A and Experimental Procedures). Despite the presence of S212D mutation in the activation loop, which results in constitutive activation of some kinases, activity analysis of the purified protein showed that the protein was catalytically inactive (Figure 2B). Crystals of the N-terminal kinase domain of MSK1 were grown as described, and the structure was determined

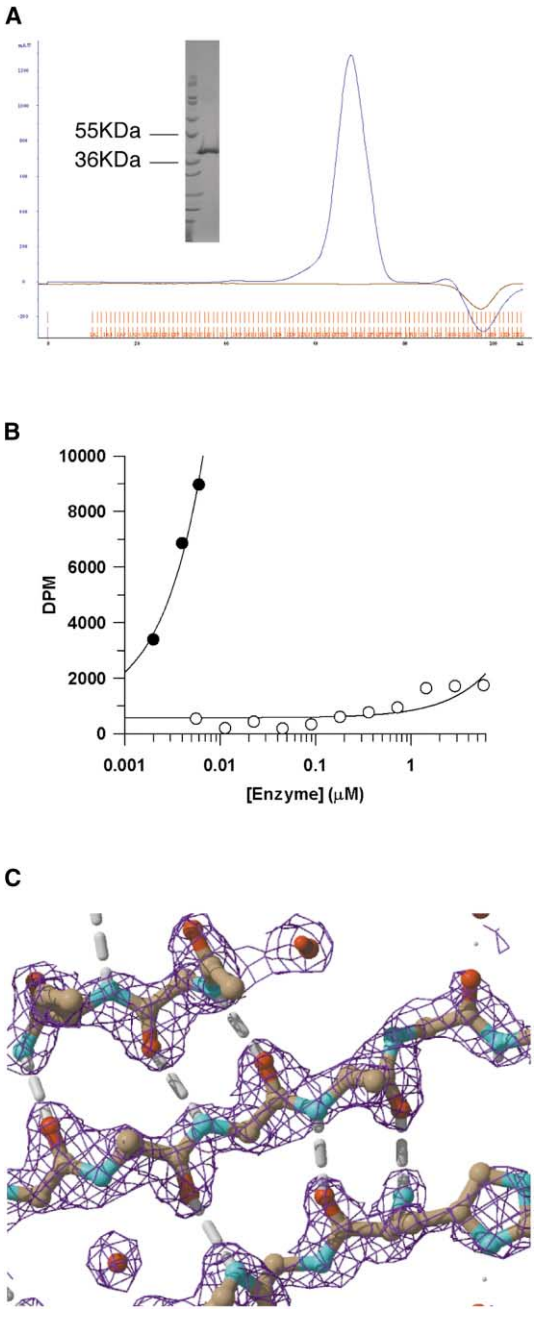

Figure 2. Protein Purification and Kinase Activity

(A) An elution profile from a Superdex200 prep grade column. The insert is a reducing SDS PAGE (Novex) gel of pure MSK1 (1-350, S212D) used for crystallization.

(B) MSK1 N-terminal domain (1-350, S212D) is inactive. Incorporation of ^{33}P into Biotin-GRPRTSSFAEG as a function of enzyme concentration under standard assay conditions (see Experimental Procedures) for full-length WT MSK1 (closed circles) and MSK1(1-350, S212D) (open circles). MSK1(1-350, S212D) is over 5000-fold less active than full-length WT MSK1.

(C) A section of electron density from the final 2fo-fc map, contoured at 1σ.

Table 1. Data Collection and Refinement Statistics

Data Collection	
Space group	$P2_12_12_1$
Molecules ASU	1
Unit cell dimensions (Å)	a = 66.62, b = 73.77, c = 89.11
Resolution (Å) (last shell)	25–1.80 (1.83–1.80)
Redundancy	4.6
I/σ (last shell)	23.6 (4.49)
Completeness (%) (last shell)	94.1 (99.9)
R_{sym}[a] (%) (last shell)	5.0 (30.7)
Wilson B (Å^2)	31.05
Refinement	
Resolution (Å) (last shell)	20–1.8 (1.85–1.80)
R_{cryst}[b] (%)	20.8 (23.8)
R_{free}[c] (%)	24.2 (28.6)
Rmsd from ideal geometry	
Bond lengths (Å)	0.013
Bond angles (°)	1.41
Main chain B (Å^2)	26.97
Average B factor protein (Å^2)	29.00
Number of atoms	
Protein atoms	2572
Solvent molecules	182
Sulphates	1

[a] $R_{sym} = \Sigma\,|I_i - \langle I\rangle|/\Sigma I_i$, where I_i is the intensity of the ith observation of a reflection and $\langle I\rangle$ is the mean intensity of the reflection.
[b] $R_{cryst} = \Sigma||F^{obs}| - |F^{cal}||/\Sigma|F^{obs}|$, where $|F^{obs}|$ and $|F^{cal}|$ are the observed and calculated structure factor amplitudes for a reflection.
[c] R_{free} was calculated from a disjoint set (10%) of reflections excluded from the refinement stages. Data between 1.98 and 1.89 Å were excluded from refinement because of an ice ring.

by molecular replacement using PKA as a search model (see Experimental Procedures). The final model has an R_{free} = 24.2% and R_{cryst} = 20.8% (Table 1; Figure 2C).

Comparison with cAMP-Dependent Kinase

The overall topology of the N-terminal kinase domain of MSK1 is similar to other protein kinases (Johnson et al., 1996) (Figure 3). The structure consists of two domains, the C-terminal lobe, which is predominantly α helical, and the N-terminal lobe, which is composed largely of β sheets. The ATP binding site is located at the interface between the two lobes while the substrate binding site is located in the C-terminal lobe centered on the activation loop. When the C-terminal lobe of MSK1 is superimposed with the C-terminal lobe of the active ternary complex of PKA (PDB code 1ATP) or active PKB (PDB code 1O6K), the rmsds are 0.93 and 1.05 Å^2 respectively [for 176 or 174 Cαs]). Compared with active PKA the N-terminal lobe of MSK1 is rotated some 12° relative to its C-terminal lobe. Several unique structural features in the N-terminal lobe of MSK1 are responsible for the inactive conformation of the kinase (Figure 3).

The Nucleotide Binding Loop and Activation Loop

Compared with the structure of active PKA and the active conformation of other protein kinases, the ATP binding site of MSK1 is sterically blocked by the nucleotide binding loop (red, Figures 3A and 3C). In active PKA, the nucleotide binding loop is positioned to allow access of ATP to the interface between the N- and C-terminal lobes, and contributes to the optimal positioning of ATP for phosphate transfer to substrate (Figure 3C). In MSK1, the conformation of the nucleotide binding loop occludes the ATP binding site (Figure 3A). The side chain of Tyr60 (B factor 38 Å^2) in the nucleotide binding loop of MSK1 occupies the adenine binding site (Figure 4A). The tyrosine hydroxyl group does not form any hydrogen bonds and is located in a predominantly hydrophobic environment, within 4 Å of residues Val115, Thr194, and Leu131. Conserved lysine residue 81, which coordinates the β-phosphate of ATP in a catalytically active kinase, hydrogen bonds to the main chain carbonyl of Tyr60. In this inactive conformation of MSK1, there is not enough room for ATP to bind in the ATP binding site. This is consistent with activity studies showing that MSK1 (1-350, S212D) is inactive (Figure 2B).

The activation loop of MSK1 also adopts a unique inactive conformation when compared with the conformation of a typical active kinase (blue, Figure 3). In PKA, the activation loop facilitates binding of substrate peptide and allows access to the ATP binding site (Figure 3C). In the inactive MSK1 structure presented here, the activation loop (residues 196–223, Figure 1B) is ordered (average B factor 26.9 Å^2) and packs close to the nucleotide binding loop. Residues 198–202 of the activation segment form the third strand of a unique three-stranded β sheet on the surface of the N-terminal lobe (Figure 3B). This stretch of β sheet is followed by two turns of an α helix. Residues Glu206 and Arg209 from the activation loop of MSK1 hydrogen bond to the main chain of the nucleotide binding loop (Figure 4A). Specifically, Glu206 hydrogen bonds to the mainchain nitrogen of Lys62, while Arg209 makes a water-mediated hydrogen bond to the main chain nitrogen of Ala59 (Figure 4A). The unique β strand at the beginning of the activation loop helps to position the MSK1 activation loop close to the ATP binding site and nucleotide binding loop. The close proximity of the activation loop to the nucleotide binding loop, and the hydrogen bonds that are made by Glu206 and Arg209, help to keep the MSK1 ATP binding site sterically blocked.

The αC Helix and Autoinhibitory β Sheet of MSK1

The αC helix is an important structural feature, serving to correctly align the catalytic residues in the active conformation of a kinase. Conformational changes in the αC helix are commonly observed on activation of a protein kinase (Johnson et al., 1996; Huse and Kuriyan, 2002). The AGC family of kinases also have an extra helix, the short αB helix, which precedes the αC helix and connects the αC helix with the β3 strand (Figures 1B and 3D) (Knighton et al., 1991). In MSK1, the αC helix is short, consisting of residues 101–110 which form three turns of an α helix, angled some 55° away from the αC helix in active PKA (Figures 3B and 3D). The C-terminal end of the αC helix in MSK1 is in a similar position to that in active PKA, but the N-terminal end of the αC helix has swung away from the rest of the N lobe of the kinase domain (Figures 3B and 3D). The new three-stranded β sheet in MSK1 occupies a position equivalent to the N-terminal end of the αC helix in PKA.

Inactive MSK1 does not contain an αB helix. Instead, the short αC helix is preceded by a unique β strand (βB)

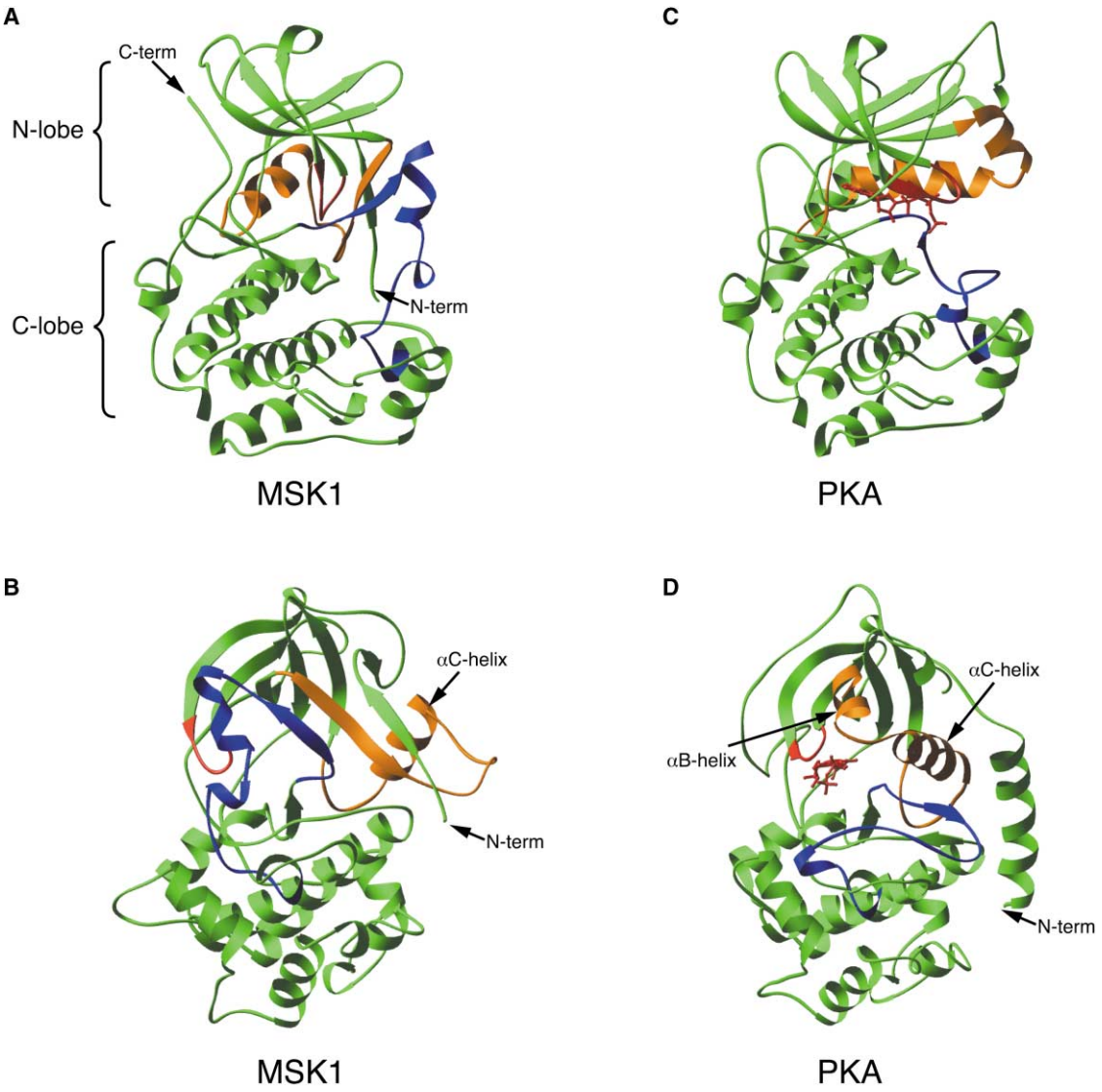

Figure 3. Overall Structure of MSK1 and PKA

(A) and (B) are ribbon diagrams of MSK1 N-terminal domain, (C) and (D) are ribbon diagrams of PKA (PDB code 1ATP) with AMP-PNP shown as red ball-and-sticks. Views (B) and (D) are of the back of the kinase and are rotated 90° relative to (A) and (C) about the vertical axis. The nucleotide binding loop of MSK1 and PKA is shown in red and the activation loop is shown in blue. The αB helix and αChelix of PKA (residues 75–104) and the equivalent residues in MSK1 (residues 84–115) are shown in orange. The three stranded β sheet motif on the surface on the MSK1 N lobe is clearly visible in (B). The three strands are from the N terminus (green), αBhelix (orange), and the activation loop (blue).

comprising residues equivalent to the αB helix (84–91) (Figures 1B and 3B). This β strand (βB) is the central strand of the new autoinhibitory three-stranded antiparallel β sheet on the surface of the N lobe (Figure 3B). This β sheet is comprised of the βB strand (equivalent to the αB helix), residues from the protein's N terminus (residues 26–32, β1L0), and the beginning of the activation loop (residues 198–202, the β9 strand) (Figures 1B and 3B). Interestingly, whereas in active kinases such as PKA the β9 strand turns down to form a β sheet with the β6 strand in the C-terminal lobe (Figure 3D), in the inactive MSK1 structure the β9 strand (198–202) turns up to take part in the new three-stranded β sheet on the N lobe (Figure 3B). This change in orientation of the β9 strand is facilitated by a different conformation of the preceeding DFG motif in MSK1 (195-197). Phe196 has rotated significantly, compared with its conformation in an active kinase, and packs against Ile108 and Leu105 from the αC helix, contributing to the inactive conformation of the αC helix. Four hydrophobic residues from the new β sheet (Leu32, Ala86, Ile88, and Leu198) are also buried and contribute to the hydrophobic core in this area.

The β sheet on the surface of the N-terminal lobe of MSK1 appears to serve two major functions in maintaining an inactive conformation of MSK1 (Figure 3B). The third strand of the β sheet (residues 198–202, from the activation loop in an active kinase), positions the activation loop close to the nucleotide binding loop so that the ATP binding site is blocked, while the middle

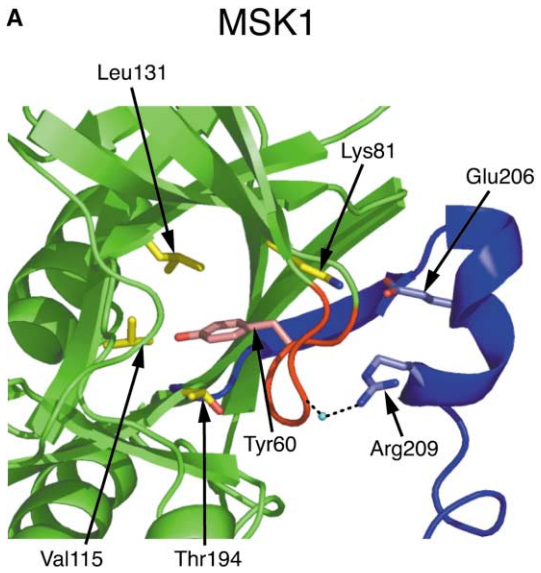

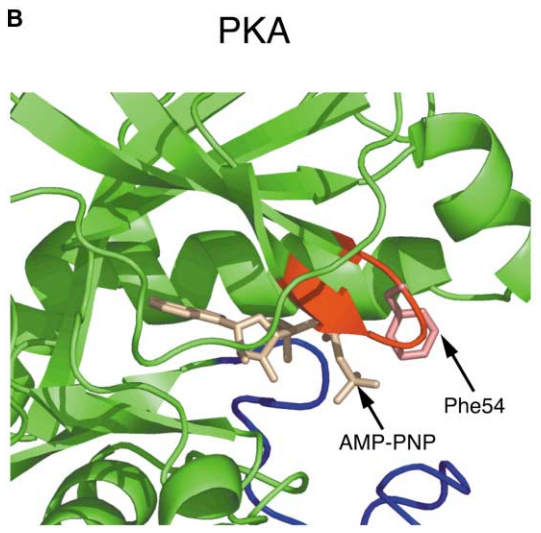

Figure 4. The Active Site of MSK1

(A) The active site of MSK1. The activation segment is shown in blue and the nucleotide binding loop is colored red. Tyr60 from the nucleotide binding loop and Glu206 and Arg209 from the activation loop are shown on the figure. Residues Leu131, Val115, Thr194 which are within 4 Å of Tyr60 are shown as well as conserved residue Lys81.

(B) The active site of PKA (PDB code 1ATP) with the nucleotide binding loop in red and the activation segment in blue. Phe 54 from the nucleotide binding loop is shown on the figure and AMP-PNP is represented in salmon as ball-and-stick.

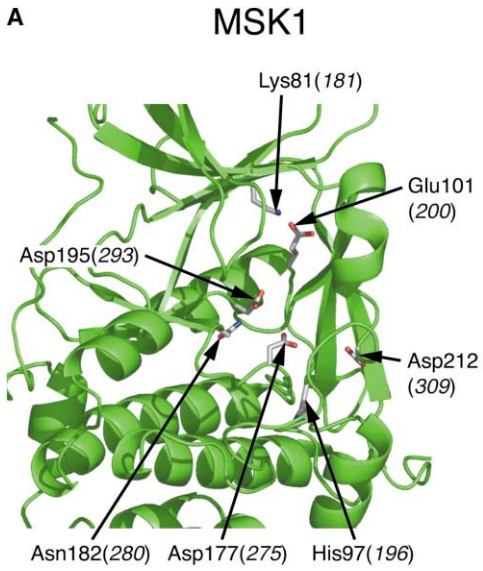

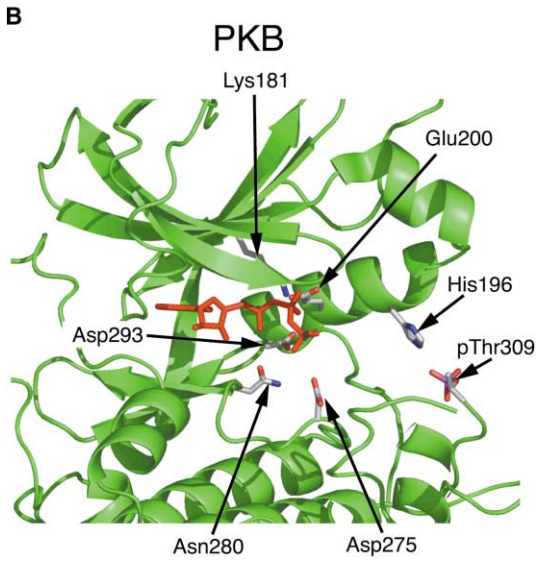

Figure 5. Catalytic Residues of MSK1 and PKB

Ribbon diagram showing the location of catalytic residues in MSK1 (A) and PKB (PDB code 1O6K, with AMP-PNP shown in red as ball-and-stick) (B). The catalytic residues are shown on both figures; in (A), the PKB numbering is shown in italics in parenthesis.

strand (residues 84–91, equivalent to the αB helix in an active AGC family kinase) locks the αC helix in an inactive conformation such that the catalytic residues are not appropriately aligned for catalysis.

Catalytic Residues

The presence of the autoinhibitory β sheet motif and the short αC helix in MSK1 cause a significant change in position of the catalytic residues (Figure 5). In an active kinase an invariant Glu in the middle of the αC helix (Glu101 in MSK1, Glu200 in PKB) accepts a hydrogen bond from a conserved Lys residue (Lys81 in MSK1, Lys181 in PKB); the conserved Lys in turn coordinates the β-phosphate of ATP (Figure 5B). In MSK1, Glu101 is solvent exposed at the end of the short αC helix and located approximately 12 Å away from the equivalent residue in active PKB (Figure 5A). MSK1 residue Lys81 is involved in a hydrogen bonding network involving the activation loop and the nucleotide binding loop (Figure 4A). In PKB, pThr309 in the activation loop is contacted by a conserved His (His196) on the αC helix (Figure 5B). In inactive MSK1, His97 (equivalent to conserved His196

in PKB) is located on the loop connecting the short αC with the autoinhibitory β sheet, approximately 23 Å away from the equivalent residue in active PKB (Figure 5A). In inactive MSK1, Ser212 in the activation loop, equivalent to Thr309 in PKB, has been mutated to Asp. In the structure described here Asp212 is partially solvent exposed and does not form any hydrogen bonds but is held in the inactive conformation of the activation segment (Figure 5A).

Comparison with Other Inactive Kinases

The structure of the inactive N-terminal kinase domain of MSK1 is most similar to that of inactive Tie2 kinase (Shewchuk et al., 2000) (Figure 6). In Tie2 kinase the ATP binding site is sterically blocked by the nucleotide binding loop; an aromatic residue (Phe23) from the nucleotide binding loop sterically occludes the binding of ATP. This is very similar to the situation observed in MSK1, with Tyr60 from the nucleotide binding loop blocking the ATP binding site. In contrast to MSK1, which has an ordered activation segment that packs close to the nucleotide binding loop, part of the activation segment of Tie2 is disordered. Interestingly, the average B factor for the MSK1 nucleotide binding loop (43 $Å^2$) is significantly higher than average for the protein (29 $Å^2$), whereas in Tie2, the average B factor of the nucleotide binding loop (24 $Å^2$) is less than average for the protein (33 $Å^2$). This raises the possibility that the conformation of the nucleotide binding loop in inactive MSK1 is unstable and held in an inactive conformation by the close proximity of the ordered activation segment.

Interestingly, MSK1 and Tie2 have autoinhibitory structures that are distinct from the inactive conformations of IRTK and PKB, where the ATP binding sites are also blocked by an aromatic residue (Huse and Kuriyan, 2002). In IRTK and PKB, the aromatic residue comes from the conserved DFG motif at the beginning of the activation loop, rather than from the nucleotide binding loop, as seen in MSK1 and Tie2 kinases. The structure of MSK1 also resembles that of kinase Abl complexed with the inhibitor STI-571 (Glivec) (Schindler et al., 2000). In this crystal structure, STI-571 binds to the inactive form of Abl, with the inhibitor packing closely against the nucleotide binding loop in a so-called "induced fit" binding mode. Although in the inactive structure of MSK1 presented here there is not enough room for ATP to bind, only a small rotation of the nucleotide binding loop is required to bind ligand (see Figure 4A). The close similarity to the inactive structure of Abl/STI-571 therefore raises the exciting possibility of designing inhibitors to the inactive conformation of MSK1 N-terminal kinase domain.

The MSK1 Hydrophobic Motif and Hydrophobic Pocket

The crystal structures of PKA, active PKB, and PDK1 reveal a hydrophobic pocket and adjacent phosphoserine/threonine docking site formed by residues from the αC helix, αB helix, and the β5 strand (Knighton et al., 1991; Yang et al., 2002a; Biondi et al., 2002) (Figure 7A). This hydrophobic pocket is characteristic of AGC family kinases and has been shown both structurally and bio-

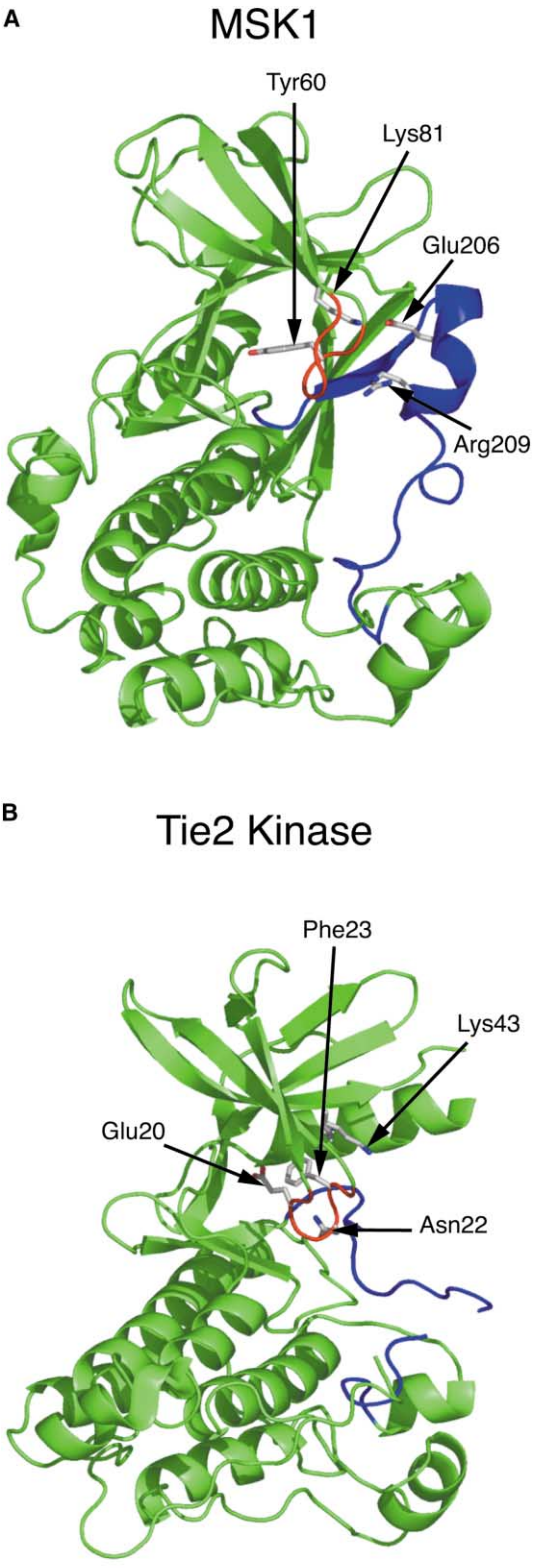

Figure 6. MSK1 and Tie2 Kinase

(A) Ribbon diagram of MSK1 showing Tyr60, Lys81, Glu206, and Arg209.

(B) Ribbon diagram of Tie2 kinase (PDB code 1FVR) showing Glu20, Phe23, Lys43, and Asn22. In both structures the nucleotide binding loop is shown in red and the activation loop in blue.

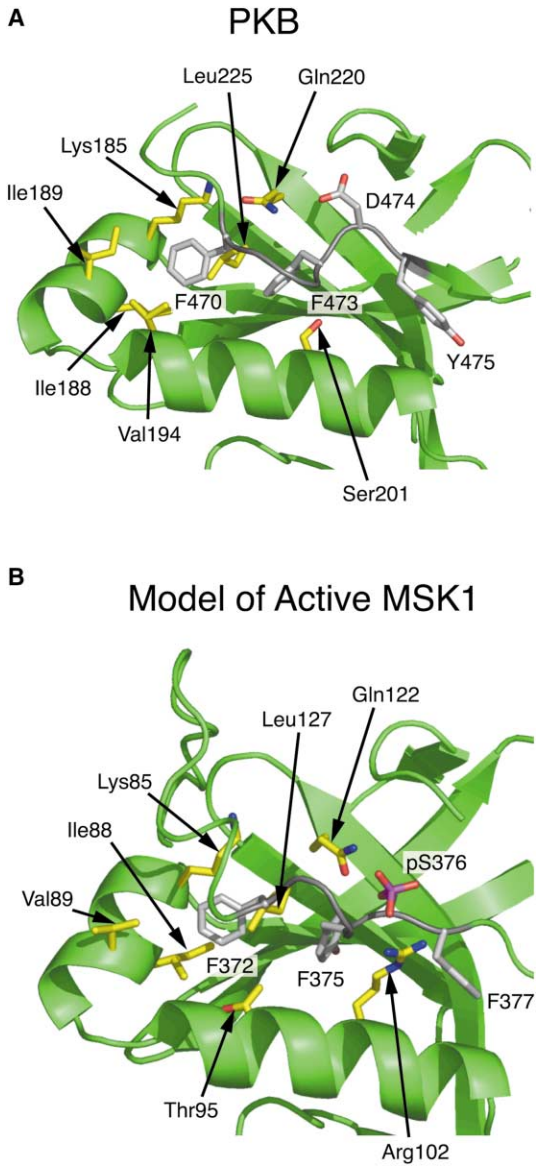

Figure 7. The Hydrophobic Groove of PKB and a Model of Active MSK1

(A) A ribbon diagram of the hydrophobic groove of active PKB (PDB code 1O6K) with the hydrophobic motif shown in gray. In this structure the phosphorylation site Ser474 has been changed to an Asp. Conserved residues Leu225, Lys185, Ile189, Ile188, and Val194 which form the hydrophobic groove are shown on the figure. Gln220 and Ser201 which form the phosphoserine/threonine docking site are also shown.

(B) A model of active MSK1 with the hydrophobic motif shown in gray. The conserved residues which form the hydrophobic groove and phosphoserine/threonine docking site (Leu127, Lys85, Ile88, Val89, Thr96, Arg102, and Gln122) are shown on the figure. The model was generated by replacing the side chains of active PKB (PDB code 1O6K) with those of MSK1.

chemically to be the binding site for regulatory phosphorylated hydrophobic motifs (Yang et al., 2002b; Frodin et al., 2002; Pearl and Barford, 2002).

For example, the recently determined crystal structures of active and inactive forms of PKB show how PKB is activated by phosphorylation of Ser474 in the C-terminal hydrophobic motif. Phosphorylation of Ser474 (mimicked by an Asp mutation in Figure 7A) results in the interaction of the phosphorylated hydrophobic motif with the hydrophobic pocket/phosphoserine docking site and the consequent burying of residues Phe470 and Phe473 (Figure 7A). PKB residues Phe470 and Phe473 are buried in a hydrophobic pocket formed by Lys185, Ile188, Ile189, Val194, and Leu225, while Asp474 hydrogen bonds to Gln220. This leads to the ordering of the αC helix, correct alignment of the catalytic residues and unblocking of the ATP binding site (previously blocked by Phe from the DFG motif).

In inactive MSK1, the hydrophobic pocket and phosphoserine docking site are not formed because the residues that would be expected to form the αB helix and part of the αC helix instead form the autoinhibitory three-stranded β sheet on the surface of the N-terminal lobe (Figures 1B and 3). Sequence comparison with other AGC family kinases, however, shows that these residues (Leu127, Lys85, Ile88, Val89, and Thr95, highlighted in yellow and green in Figure 1B) are conserved in MSK1 despite being locked in the autoinhibitory conformation described here. This strongly suggests that in the active conformation of MSK1, the hydrophobic binding pocket could be formed (see Figure 7B).

The Active Conformation of MSK1

The emerging data for the structure of the active conformation of AGC family kinases is one in which the hydrophobic motif is bound in the hydrophobic groove (Yang et al., 2002a; Biondi et al., 2000, 2002; Frodin et al., 2002). Evidence in the literature, particularly that reported by Frodin et al. (2002) suggests that this would also be the case for active MSK1. In MSK1 a conserved hydrophobic motif (FQGY**S(376)**F) is found in the linker region between the two kinase domains (Figure 1B) (Pearson et al., 1995; Frodin et al., 2000; Deak et al. 1998). This motif contains the phosphorylation site Ser376, which is believed to be autophosphorylated in active MSK1 (Williams et al., 2000; Frodin et al., 2000). Frodin et al. demonstrate the importance of the hydrophobic motif in activation of MSK1 using a reconstitution assay with the N-terminal domain of MSK1 (residues 1–370) which lacked the hydrophobic motif. Maximal kinase activity was achieved by preincubation with PDK1 (which does not phosphorylate MSK1 physiologically but can be used to phosphorylate the activation loop in vitro) and incubation with pHM^{s6k}. These experiments suggest that for MSK1 the phosphorylated hydrophobic motif stimulates kinase activity synergistically with phosphorylation of the activation loop in the N-terminal kinase domain. These experiments also show that mutation of MSK1 residue Arg102, located in the putative phosphoserine binding site/hydrophobic groove, prevents in vivo activation of full-length protein as well as preventing activation of the N-terminal domain in the reconstitution assay.

The active conformation of all kinases studied to date adopt a similar overall tertiary structure (Johnson et al., 1996). It would therefore be very surprising if the active conformation of MSK1 differed significantly from the

structure of other active kinases. We replaced the side chains of active PKB with those of MSK1 to see if it is feasible for MSK1 to adopt an active conformation consistent with that of a representative active AGC family kinase (Figure 7B). Figure 7B shows that it is possible for MSK1 to adopt a conformation similar to the active conformation observed in a typical AGC family kinase; furthermore, it is possible for the linker region of MSK1, including the phosphorylated hydrophobic motif, to bind on the surface of the N-terminal lobe in a conformation similar to that observed for active PKB (and PKA). As previously discussed, the residues (Leu127, Lys85, Ile88, Val89, Thr95, Gln122, and Arg102) that are needed to form the hydrophobic binding pocket and phosphoserine docking site are conserved in MSK1 (Figure 1B). This includes residue Arg102, which has been shown to be essential for activation of full-length MSK1 (Frodin et al., 2002).

Discussion

We present here the structure of a novel autoinhibitory conformation for the N-terminal kinase domain of MSK1. The hydrophobic binding pocket normally found in the active AGC family of kinases includes residues from the αB helix. In the inactive structure of MSK1, residues which normally form the αB helix in the active conformation now adopt a β strand conformation. These residues form part of a novel three-stranded β sheet, together with residues from the N terminus and the activation loop. The presence of the three-stranded β sheet contributes to the inactive conformation of MSK1 in two major ways. First, both the short αC helix and β sheet result in significant misalignment of the catalytic residues. Second, the presence of the β sheet helps to keep the activation loop and nucleotide binding loop in a conformation where the ATP binding site is sterically blocked by a tyrosine residue (Tyr60) from the nucleotide binding loop (Figures 3 and 5). The presence of the β sheet in the N lobe of MSK1 N-terminal kinase is a unique structural feature that has not previously been observed and represents a novel autoinhibitory mechanism for this dual domain kinase.

As the active conformation of all protein kinases determined to date adopt a similar overall tertiary structure (Johnson et al., 1996), it would be very surprising if the active conformation of MSK1 did not also adopt such a tertiary conformation. Biochemical data reported in the literature for MSK1 is consistent with a tertiary structure similar to that observed for other active kinases (Frodin et al., 2002). In addition, and consistent with the emerging story for AGC family kinases, biochemical data for MSK1 also indicates a role for the hydrophobic motif, located in the linker region between the N- and C-terminal kinase domains, in the activation of full-length kinase. Taken together, this would imply that large conformation changes in the nucleotide binding loop, activation segment, and αC helix would be necessary to fully activate the N-terminal kinase domain of MSK1. The recently determined crystal structures of active and inactive forms of PKB (Yang et al., 2002a, 2002b) show that large conformational changes are necessary to activate this AGC family kinase, therefore setting a precedent for this type of activation. The exact role of the C-terminal kinase domain of MSK1 in activation of full-length protein remains to be established.

Experimental Procedures

Cloning and Expression

The MSK1 1-350 truncate was generated by PCR from a full-length cDNA clone (kindly provided by DSTT, University of Dundee [Deak et al., 1998]). A His_6 tag was added at the N terminus and BamHI/XhoI restriction sites at the 5′ and 3′, respectively. The PCR product was subcloned into BamHI/XhoI digested pFASTBAC1. The S212D mutation was introduced using Stratagene QuickChange mutagenesis kit according to the manufacturer's instructions. The MSK1 expression cassette was then transposed into the parent bacmid using the Invitrogen Bac-to-Bac system. Purified bacmids were transfected into Sf-9 cells using cellfectin. Initial virus stocks were harvested 3 days posttransfection, and high titre virus stocks were generated by infection of fresh Sf9 cultures and incubation at 27°C, 100 rpm for 5 days. The high titre virus stock was used to infect expression cultures.

Purification of the N-Terminal Kinase Domain of MSK1 (1-350, S212D)

2.24×10^{10} baculovirus-infected Sf-9 cells were resuspended in 600 ml of buffer A (10 mM HEPES, pH 7.5, 300 mM NaCl, 5 mM NaPyrophosphate, 1 mm NaOrthovanadate, 10 mM NaF, 1 mM β-glycerophosphate, 10 mM β-mercaptoethanol, 10% glycerol, 0.1 mM EDTA, 0.1 mM EGTA) and disrupted by dounce homogenization, on ice. The insoluble material was removed by centrifugation at 48,000 × g for 90 min at 4°C. The supernatant was contacted with 30 ml of NiNTA Superflow (Qiagen) for 16 hr at 4°C. The NiNTA was recovered by centrifugation, packed into a column (XK26 Amersham Biosciences), and eluted using 300 ml of lysis buffer A, 300 ml buffer A + 1 M NaCl, 300 ml buffer A + 20 mM imidazole, and 300 ml buffer + 300 mM imidazole using an AKTA Purifier 100 (Amersham Biosciences). The three fractions from the 300 mM imidazole elution containing the MSK1 were pooled and buffer exchanged using a 275 ml G25M column (XK50 Amersham Biosciences) into buffer B (20 mM Tris, pH 8.0, 10 mM NaCl, 10 mM β-McEtOH, 10% glycerol, complete EDTA free, 1 mM EDTA). The buffer exchanged material was 0.45 μm filtered and loaded directly on to a 20 ml Source 15Q column (HR16/10 Amersham Biosciences), the column was eluted using a linear NaCl gradient from 10 to 500 mM NaCl over 50 bed volumes collecting 10 ml fractions using an AKTA Purifier 100 (Amersham Biosciences). The MSK1 eluted as a single peak at around 150–200 mM NaCl. The MSK1 was pooled and concentrated by ultrafiltration to a final volume of 5 ml and loaded on to a 100 ml Superdex200 prep grade cloumn (HR16/60 Amersham Biosciences) that had been equilibrated in buffer B containing 250 mM NaCl, the column was eluted using 1.2 bed volumes of buffer collecting 1 ml fractions, using an AKTA Purifier100 (Amersham Biosciences). The MSK1 eluted as a single peak at the expected molecular weight for monomeric protein. The MSK1 containing fractions, eluted between 64 and 74 ml, were pooled and concentrated to 10 mg/ml by untrafilration, yielding a total of 124 mg of pure MSK1. Analysis by LC-MS (LCT Waters/Micromass) gave a mass of 39,822 Da, exactly as predicted from the protein sequence.

Enzyme Activity

Enzyme activity was assayed by incorporation of ^{33}P into a CREB-derived peptide substrate. Enzyme (typically 2 nM for full-length WT MSK1 activated by MAPK2) was incubated with Biotin-GRPRTS SFAEG (2 μM) and ^{33}P ATP (20 μM, 500 kBq/ml) in assay buffer (50 mM HEPES, pH 7.5, 10 mM $MgCl_2$, 0.1 mM EGTA, 0.01% Tween-20, 5 mM β-mercaptoethanol, 2.5% DMSO) for 60 min at room temperature in white 384-well NUNC plates. The assay was stopped by the addition of EDTA (to 50 mM) and 2.5 mg/ml Steptavidin PVT SPA beads. Plates were then read on a Wallac Trilux.

Crystallization and Data Collection

MSK1 crystals were grown by vapor diffusion at 20°C using protein at a concentration of 5.75 mg/ml (in 5 mM Tris, pH 8.0, 62 mM NaCl, 0.25 mM NaOrthovanadate, 2.5 mM β-McEtOH, 2.5% glycerol, 0.025 mM EDTA, 0.05 mM PMSF, 0.25 mM benzamidine) and well solution of 2.0 M ammonium sulfate, 0.1 M Tris, pH 8.5. Crystals appeared overnight and grew to full size (150 × 50 × 50 μM) in 2–3 days. For freezing, crystals were transferred to cryo-buffer and then frozen by dunking into liquid nitrogen. Cryo-buffer consisted of well solution with glycerol to a final concentration of 20%. Data was collected at the ESRF on station 14.2 and processed and scaled using DENZO and SCALEPACK (Otwinowski, 1993). See Table 1 for data collection statistics.

Structure Determination and Refinement

The structure was determined by molecular replacement using the program AMORE (CCP4, 1994) and cAMP-dependent kinase (PDB entry 1ATP) as a search model. The search model consisted of residues 40–300. The correct solution was the top peak in both the rotation (correlation coefficent = 15.3) and translation functions (correlation coefficicent = 26.1). Rigid body refinement, minimization, and individual B factor refinement using CNX (Brunger et al., 1998) gave an R_{free} = 51.0% and R_{work} = 47.2%. Residues that were not conserved between the search model and MSK1 were then changed to alanine and subsequent minimization; individual B factor refinement and simulated annealing gave R_{free} = 45.5% and R_{work} = 43%. Electron density maps were then calculated and clearly showed that the solution was correct. Iterative rounds of model building in "O" (Jones et al., 1991) and refinement in CNX and finally Refmac (Murshudov et al., 1997) were then carried out to give the final model with an R_{free} = 24.2% and R_{work} = 20.8% (See Table 1 for full refinement statistics). As a final check we ran ArpWarp (Perrakis et al., 1999) on the trimmed down molecular replacement solution which confirmed the novel parts of the structure. The first 23 residues and the N-terminal histidine tag are disordered and have not been included in the final model. Residues 230–232 are also disordered and have not been included in the final model and residues 340–345 have been built in as alanine. Figure 3 was generated with RIBBONS (Carson, 1991). Figures 2C, 4, 5, 6, and 7 were generated with PYMOL (DeLano, 2002). The model of active MSK1 was generated using the program "O" and is based on the structures of active PKA and PKB.

Acknowledgments

The authors would like to thank Lisa Shewchuk for critical reading of the manuscript, the staff at the ESRF for help with data collection, and DSTT University of Dundee for provision of full-length MSK1 cDNA clone.

Received: October 27, 20003
Revised: February 3, 2004
Accepted: February 12, 2004
Published: June 8, 2004

References

Arthur, J.S., and Cohen, P. (2000). MSK1 is required for CREB phosphorylation in response to mitogens in mouse embryonic stem cells. FEBS Lett. *482*, 44–48.

Balendran, A., Biondi, R.M., Cheung, P.C., Casamayor, A., Deak, M., and Alessi, D.R. (2000). A 3-phosphoinositide-dependent protein kinase-1 (PDK1) docking site is required for the phosphorylation or protein kinase C z (PKCz) and PKC-related kinase 2 by PDK1. J. Biol. Chem. *275*, 20806–20813.

Biondi, R.M., Cheung, P.C., Casamayor, A., Deak, M., Currie, R.A., and Alessi, D.R. (2000). Identification of a pocket in the PDK1 kinase domain that interacts with PIF and the C-terminal residues of PKA. EMBO J. *19*, 979–988.

Biondi, M., Komander, D., Thomas, C., Lizcano, J., Deak, M., Alessi, D.R., and Aalten, D.M. (2002). High resolution crystal structure of the human PDK1 catalytic domain defines the regulatory phosphospeptide docking site. EMBO J. *21*, 4219–4228.

Bjorbaek, C., Zhao, Y., and Moller, D.E. (1995). Divergent roles for p90 (RSK) kinase domains. J. Biol. Chem. *270*, 18848–18852.

Brunger, A., Adams, P.D., and Clore, G.M. (1998). Crystallography & NMR system: a new software suite for macromolecular structure determination. Acta Crystallogr. D Biol. Crystallogr. *54*, 905–921.

Carson, M. (1991). Ribbons 2.0. Appl. Crystallogr. *24*, 958–961.

CCP4 (Collaborative Computational Project 4) (1994). The CCP4 suite: programs for protein crystallography. Acta Crystallogr. D *50*, 760–763.

Chen, R.H., Sarnecki, C., and Blenis, J. (1992). Nuclear localization and regulation of erk- and rsk-encoded protein kinases. Mol. Cell. Biol. *12*, 915–927.

Dalby, K.N., Morrice, N., Caudwell, F.B., Avruch, J., and Cohen, P. (1998). Identification of regulatory phosphorylation sites in mitogen-activated protein kinase (MAPK)-activated protein kinase-1a/p90 (RSK) that are inducible by MAPK. J. Biol. Chem. *273*, 1496–1505.

Deak, M., Clifton, A., Lucocq, J., and Alessi, D. (1998). Mitogen- and stress-activated protein kinase-1 (MSK1) is directly activated by MAPK and SAPK2/p38, and may mediate activation of CREB. EMBO J.*17*, 4426–4441.

DeLano, W.L. (2002). The Pymol Molecular Graphics System (San Carlos, CA: DeLano Scientific).

Fisher, T.L., and Blenis, J. (1996). Evidence for two catalytically active kinase domains in pp90rsk. Mol. Cell. Biol. *16*, 1212–1219.

Frodin, M., Jensen, C.J., Merienne, K., and Gammeltoft, S. (2000). A phosphoserine-regulated docking site in the protein kinase RSK2 that recruits and activates PDK1. EMBO J. *19*, 2924–2934.

Frodin, M., Antal, T.L., Dummler, B.A., Jensen, C.J., Deak, M., Gammeltoft, S., and Biondi, M. (2002). A phosphoserine/threonine-binding pocket in AGC kinases and PDK1 mediates activation by hydrophobic motif phosphorylation. EMBO J. *21*, 5396–5407.

Huang, X., Begley, M., Morgenstern, K.A., Gu, Y., Rose, P., Zhao, H., and Zhu, X. (2003). Crystal structure of an Inactive Akt2 Kinase Domain. Structure *11*, 21–30.

Huse, M., and Kuriyan, J. (2002). The conformational plasticity of protein kinases. Cell *109*, 275–282.

Janknecht, R. (2003). Regulation of the ER81 transcription factor and its coactivators by mitogen- and stress- activated protein kinase 1 (MSK1). Oncogene *22*, 746–755.

Jensen, C.J., Buch, M.-B., Krag, T.O., Hemmings, B.A., Gammeltoft, S., and Frodin, M. (1999). 90kDa ribosomal S6 kinase (RSK) is phosphorylated and activated by 3-phosphoinositide-dependent protein kinase-1 (PDK1). J. Biol. Chem. *274*, 27168–27176.

Johnson, L.N., Noble, M.E., and Owen, D.J. (1996). Active and inactive protein kinases: structural basis for regulation. Cell *85*, 149–158.

Jones, T., Zou, J.-Y., and Cowan, S. (1991). Improved methods for building protein models in electron density maps and the location of errors in these models. Acta Crystallogr. A *47*, 110–119.

Knighton, D.R., Zheng, J.H., Ten Eyck, L.F., Ashford, V.A., Xuong, N.H., Taylor, S.S., and Sowadski, J.M. (1991). Crystal structure of the catalytic subunit of cyclic adenosine monophosphate-dependent protein kinase. Science *253*, 407–414.

Lodowski, D.T., Pitcher, J.A., Capel, W.D., Lefkowitz, R.J., and Tesmer, J.J.G. (2003). Keeping G proteins at bay: a complex between G protein-coupled receptor kinase 2 and Gβγ. Science *300*, 1256–1262.

Markou, T., and Lazou, A. (2002). Phosphorylation and activation of mitogen- and stress-activated kinase-1 in adult rat cardiac myocytes by G-protein-coupled receptor agonists requires both extracellular-signal-regulated kinase and p38 mitogen-activated protein kinase. Biochem. J. *365*, 757–763.

Murshudov, G.N., Vagin, A.A., and Dodson, E.J. (1997). Refinement of macromolecular structures by the maximum likelihood method. Acta Crystallogr. D *53*, 240–255.

New, L., Zhao, M., Li, Y., Bassett, W.W., Feng, Y., Ludwig, S., Padova, F.D., Gram, H., and Han, J. (1999). Cloning and characterisation

of RLPK, a novel RSK-related protein kinase. J. Biol. Chem. *274*, 1026–1032.

Otwinowski, Z. (1993). Data collection and processing. In Proceedings of CCP4 Study Weekend, L. Sawyer, N. Isaacs, and S. Bailey, eds. (Warrington, UK: SERC Daresbury Laboratory), pp. 56–62.

Pearl, L., and Barford, D. (2002). Regulation of protein kinases in insulin, growth factor and Wnt signalling. Curr. Opin. Struct. Biol. *12*, 761–767.

Pearson, R.B., Dennis, P.B., Han, J.W., Williamson, N.A., Kozma, S.C., Wettenhall, R.E., and Thomas, G. (1995). The principle target of rapamycin-induced p70s6k inactivation is a novel phosphorylation site within a conserved hydrophobic motif. EMBO J. *14*, 5279–5287.

Perrakis, A., Morris, R., and Lamzin, V.S. (1999). Automated protein model building combined with iterative structure refinement. Nat. Struc. Biol. *6*, 458–463.

Pierrat, B., Correia, J.S., Mary, J.L., Tomas-Zubar, M., and Lesslauer, W. (1998). RSK-B, a novel ribosomal S6 kinase family member, is a CREB kinase under dominant control of p38alpha mitogen-activated protein kinase (p38alphaMAPK). J. Biol. Chem. *273*, 29661–29671.

Richards, S.A., Fu, J., Romanelli, A., Shimamura, A., and Blenis, J. (1999). Ribosomal S6 kinase 1 (RSK1) activation requires signals dependent on and independent of the MAP kinase ERK. Curr. Biol. *9*, 810–820.

Schindler, T., Bornmann, W., Pellicena, P., Miller, W.T., Clarkson, B., and Kuriyan, J. (2000). Structural mechanism for STI-571 inhibition of abelson tyrosine kinase. Science *289*, 1938–1942.

Shewchuk, L., Hassell, A.M., Ellis, B., Holmes, W.D., Davies, R., Horne, E., Kadwell, S.H., McKee, D.D., and Moore, J.T. (2000). Structure of the Tie2 RTK domain: self-inhibition by the nucleotide binding loop, activation loop and C-terminal tail. Structure *8*, 1105–1113.

Song, K.S., Lee, W.J., Chung, K.C., Koo, J.S., Yang, E.J., Choi, J.Y., and Yoon, J.H. (2003). IL-1 beta and TNF alpha induce MUC5AC overexpression through a mechanism involving ERK/p38 MAP kinases-MSK1-CREB activation in human airway epithelial cells. J. Biol. Chem. *278*, 23243–23250. Published online April 10, 2003. 10.1074/jbc.M300096200

Thompson, S., Clayton, A.L., Hazzalin, C.A., Rose, S., Barratt, M.J., and Mahadevan, L.C. (1999). The nucleosomal response associated with immediate-early gene induction is mediated via alternative MAP kinase kinase cascades:MSK1 as a potential H3/HMG-14 kinase. EMBO J. *18*, 4779–4793.

Vermeulen, L., Wilde, G., Damme, P.V., Berghe, W.V., and Haegeman, G. (2003). Transcriptional activation of the NF-kB p65 subunit by mitogen-and stress-activated protein kinase-1 (MSK1). EMBO J. *22*, 1313–1324.

Vik, T.A., and Ryder, J.W. (1997). Identification of serine 380 as the major site of phosphorylation of *Xenopus* pp90rsk. Biochem. Biophys. Res. Commun. *235*, 398–402.

Wiggin, G.R., Soloaga, A., Foster, J.M., Murray-Tait, V., Cohen, P., and Arthur, J.S. (2002). MSK1 and MSK2 are required for the mitogen- and stress- induced phosphorylation of CREB and AFT1 in fibroblasts. Mol. Cell. Biol. *22*, 2871–2881.

Williams, M.R., Arthur, J.S., Balendran, A., Van der Kaay, J., Poli, V., Cohen, P., and Alessi, D.R. (2000). The role of 3-phosphinositide-dependent protein kinase 1 in activating AGC kinases defined in embryonic stem cells. Curr. Biol. *10*, 439–448.

Yang, J., Cron, P., Thompson, V.M.G., Hess, D., Hemmings, B.A., and Barford, D. (2002a). Molecular mechanism for the regulation of protein kinase B/Akt by hydrophobic motif phosphorylation. Mol. Cell *9*, 1227–1240.

Yang, J., Cron, P., Good, V., Thompson, V., Hemmings, B.A., and Barford, D. (2002b). Crystal structure of an activated Akt/protein kinase B ternary complex with GSK3-peptide and AMP-PNP. Nat. Struct. Biol. *9*, 940–944.

Zhao, Y., Bjorbaek, C., Weremowicz, S., Morton, C.C., and Moller, D.E. (1995). RSK3 encodes a novel pp90rsk isoform with a unique N-terminal sequence; growth factor-stimulated kinase function and nuclear translocation. Mol. Cell. Biol. *15*, 4353–4363.

Zhong, S., Jansen, C., She, Q.B., Goto, H., Inagaki, M., Bode, A.M., Ma, W.Y., and Dong, Z. (2003). Ultrviolet B-induced phosphorylation of histone H3 at serine 28 is mediated by MSK1. J. Biol. Chem. *276*, 33213–33219.

Accession Numbers

The coordinates have been deposited in the PDB (code 1vzo).